Optica Applicata, Vol. XLVIII, No. 3, 2018
10.5277/oa180315

A fast dehazing method with high color fidelity

YILIN SHAN[1, 2], PENG GE[1]

[1]Engineering Research Center for Optoelectronics of Guangdong Province, School of Physics and Optoelectronics, South China University of Technology, Guangzhou 510640, China

[2]Guangdong Provincial Key Laboratory of Precision Equipment and Manufacturing Technology, School of Mechanical and Automotive Engineering, South China University of Technology, Guangzhou, 510640, China

In this paper, we present a fog image degradation model with the combination of HSI color space and the atmosphere scattering model. Based on the model, a fast dehazing method with high color fidelity has been proposed. The main advantage of the proposed method compared with others is its speed. This speed allows the method to be applied within real-time processing applications as a step of preprocessing. Another advantage is the possibility to handle both color images and gray level images. The algorithm depends only on on two parameters, and both are easy to set. Experiments on haze images demonstrate that the proposed method can achieve wonderful image visibility with a higher computing speed.

Keywords: digital image processing, atmospheric scattering, dehazing.

1. Introduction

Images of outdoor scenes taken on foggy days are greatly degraded by suspended particles in the atmosphere. It affects normal function of outdoor imaging equipment. So the haze removal algorithm is highly desired in outdoor imaging.

Early dehazing methods need multiple images of the same scene under different weather conditions [1–3] or some additional information [4–6]. Due to the harsh condition requirements, these methods are difficult to be applied in real-time equipment.

Recently, single image haze removal [7, 8] has achieved significant progresses. Tan's method, Fattal's method and He's method [9–11] are the most popular algorithms. All these methods take a prior or assumption to obtain haze-free images. Compared with other methods, He's method based on a data statistical prior is more reliable with a better visual result. However, a soft matting, an important step in He's method, is time-consuming. Many improved algorithms appeared to increase the efficiency of dark channel prior. And KAIMING HE *et al*. also proposed an efficient guided image filter [12] to re-

place soft matting. Although much progress has been done to improve the computing speed of the algorithm, the step of figuring out the medium transmission item is still time-consuming. Furthermore, the methods cannot process gray level images.

In this paper, a novelty fog image degradation model in HSI color space has been proposed. The medium transmission item has been eliminated in the model. Moreover, the model shows a close relationship between the intensity component and saturation component. So based on the model, we can remove haze efficiently with a vivid result. In addition, the method can also handle gray level images.

2. A novelty fog image degradation model in HSI color space

The degradation process in foggy days can be described as follows [10, 11]:

$$I(x) = J(x)t(x) + A(1 - t(x)) \tag{1}$$

where $I(x)$ is the observed intensity of the input foggy image, $J(x)$ is the underlying haze-free image, A is the global atmospheric light, and $t(x)$ is the medium transmission.

The HSI color space is based on the cylindrical coordinate system, and the conversion from RGB color space to HSI color space is described as:

$$H = \cos^{-1}\left\{ \frac{\left[(R-G)+(R-B)\right]/2}{\sqrt{(R-G)^2+(R-B)(G-B)}} \right\} \tag{2}$$

$$S = 1 - \frac{3}{R+G+B}\min(R, G, B) \tag{3}$$

$$I = \frac{R+G+B}{3} \tag{4}$$

Actually, the value of medium transmission $t(x)$ and the global atmospheric light A are almost the same for all RGB channels. In this paper, we assume $t(x)$ and A are the same for all RGB channels.

To obtain the relationship of a hue component between the hazy image and the underlying haze-free image, we combined Eq. (1) and Eq. (2):

$$H_{\mathrm{I}} = H_{\mathrm{J}} \tag{5}$$

where H_{I} is the hazy image's hue component and H_{J} is the underlying haze-free image's hue component. Equation (5) proves that the haze cannot affect the hue component.

Here we separate Eq. (1) into the R, G, B channels and sum them up

$$I_{\mathrm{R}} + I_{\mathrm{G}} + I_{\mathrm{B}} = (J_{\mathrm{R}} + J_{\mathrm{G}} + J_{\mathrm{B}})t + 3A(1 - t) \tag{6}$$

According to Eq. (4), Eq. (6) can be transformed into

$$I_{\mathrm{I}} = I_{\mathrm{J}} t + A(1 - t) \tag{7}$$

where I_{I} is the hazy image's intensity component, I_{J} is the underlying haze-free image's intensity component. Then we take the minimum operation among three color channels in Eq. (1) and get

$$I_{\min(R,\,G,\,B)} = J_{\min(R,\,G,\,B)}\, t + A(1 - t) \tag{8}$$

By subtracting Eq. (8) from Eq. (7):

$$I_{\mathrm{I}} - I_{\min(R,\,G,\,B)} = (I_{\mathrm{J}} - J_{\min(R,\,G,\,B)})\, t \tag{9}$$

Actually, compared with Eq. (3), Eq. (9) can be simplified as

$$S_{\mathrm{I}} = \frac{S_{\mathrm{J}} I_{\mathrm{J}} t}{I_{\mathrm{I}}} \tag{10}$$

Finally, we get a series of equations which has been proposed by Xiang *et al*. [13]:

$$\begin{cases} H_{\mathrm{I}} = H_{\mathrm{J}} \\ S_{\mathrm{I}} = \dfrac{S_{\mathrm{J}} I_{\mathrm{J}} t}{I_{\mathrm{I}}} \\ I_{\mathrm{I}} = I_{\mathrm{J}} t + A(1 - t) \end{cases} \tag{11}$$

Based on Eqs. (11), Xiang proposed a dehazing method. In fact, Xiang's method is very similar to He's method. He's method is based on the dark channel prior while Xiang's method is based on the full-saturation assumption. The former describes that the minimum intensity in an outdoor haze-free image within a local patch should have a very low value close to 0. The latter describes that the maximum saturation in a macroblock of an image should have a very high value close to 1. It can be viewed as different forms in RGB color space and HSI color space of the same property. And both methods need to figure out medium transmission $t(x)$, which is time-consuming.

To eliminate medium transmission $t(x)$, we put Eq. (7) into Eq. (10) and obtain

$$S_{\mathrm{J}} = k\left(\frac{A - I_{\mathrm{J}}}{I_{\mathrm{J}}}\right) \tag{12}$$

where $k = \dfrac{S_{\mathrm{I}} I_{\mathrm{I}}}{A - I_{\mathrm{I}}}$.

Combining Eq. (3) and Eq. (12)

$$I_{\mathrm{J}} = \frac{kA + J_{\min(R,\,G,\,B)}}{1+k} \tag{13}$$

Then we get a novelty fog image degradation model in HSI color space:

$$\begin{cases} H_{\mathrm{J}} = H_{\mathrm{I}} \\ S_{\mathrm{J}} = k\left(\dfrac{A - I_{\mathrm{J}}}{I_{\mathrm{J}}}\right) \\ I_{\mathrm{J}} = \dfrac{kA + J_{\min(R,\,G,\,B)}}{1+k} \end{cases} \tag{14}$$

The nice property of this model is that once $J_{\min(R,\,G,\,B)}$ is figured out, we can use Eq. (14) to obtain the whole haze-free image without the process of solving $t(x)$.

In a traditional atmospheric scattering model, we recover a hazy image in RGB color space. The process of recovery is independent in each channel. Deviation of $t(x)$ might lead to independent deviation among three channels, furthermore, the results may appear as serious color distortion. So the accuracy of medium transmission $t(x)$ is very important in the traditional model. According to Eq. (14), the hue component is only decided by haze image's hue component in our model, moreover, the saturation component and intensity component are closely related. The saturation component would change with the change of intensity, and the results can still be natural. So the accuracy of $J_{\min(R,\,G,\,B)}$ is less significant in our model. The relationship between the saturation component and the intensity component ensures that the results can still keep visually-pleasant even when $J_{\min(R,\,G,\,B)}$ has a large deviation. As in Fig. 1, we use another $J_{\min(R,\,G,\,B)}$ with a totally different histogram to replace original $J_{\min(R,\,G,\,B)}$, the results are almost the same as the original image.

3. Haze removal using our fog image degradation model

3.1. Estimating the intensity component

In this paper, the histogram matching method, a simple but efficient algorithm, is taken to estimate $J_{\min(R,\,G,\,B)}$. To estimate the object histogram 200 outdoor photos (100 photos without sky area, 100 photos with sky area) were used. Because the sky in a hazy day is always white not blue, we only selected photos with the white sky as statistical samples. The statistical results were used as the matching objects in histogram matching process. As shown in Fig. 2**a** and 2**b**, some intensity value's probability in the statistical histogram were extremely high. This might lead to less gray level of results' histogram and concentrated distribution in some gray level. Moreover, the results would lose lots of details. The revise has been taken on the statistical histogram in Figs. 1**f** and 1**h**. In

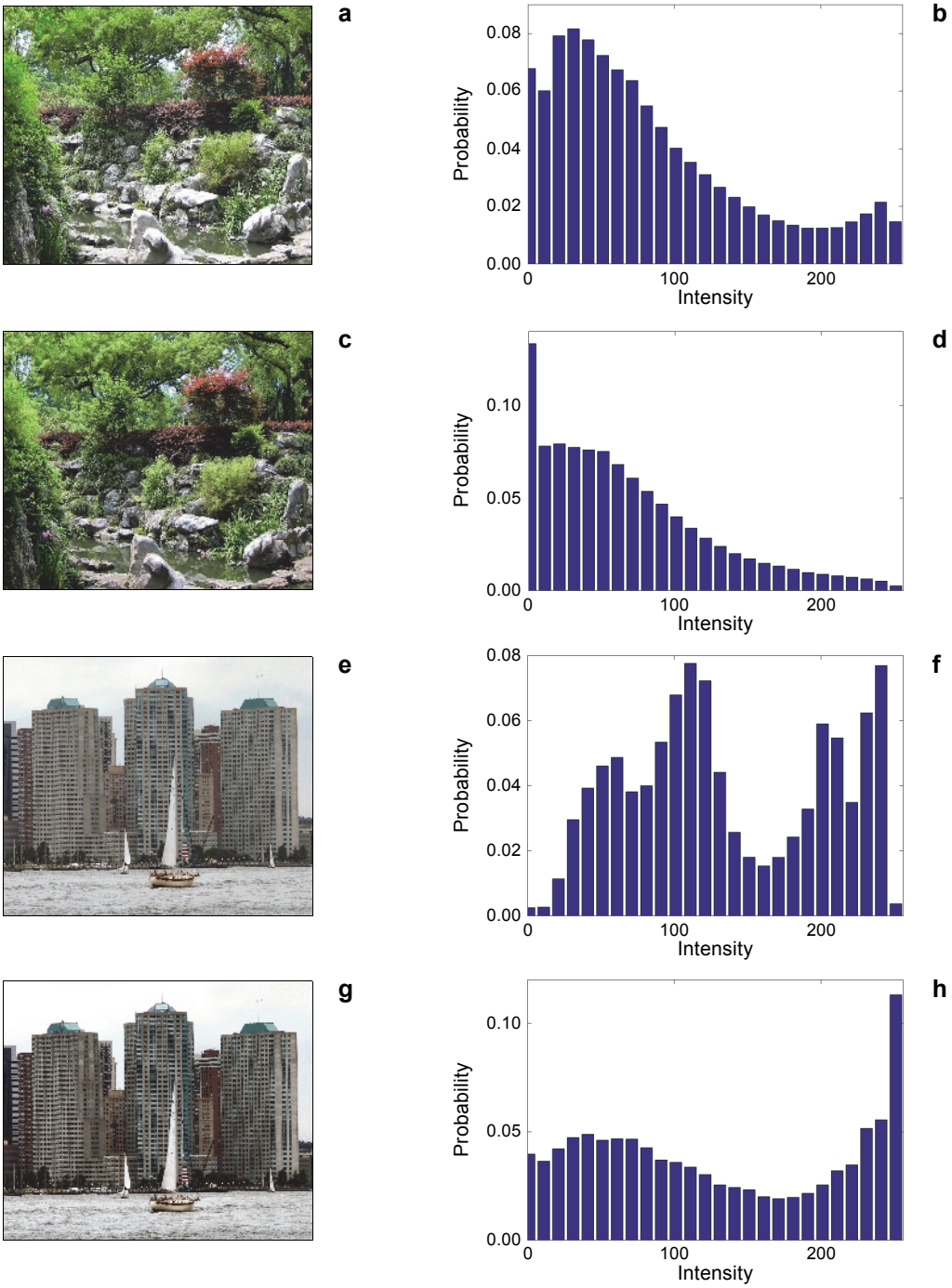

Fig. 1. Original "non-sky" image (**a**), and the histogram of its $J_{\min(R,\ G,\ B)}$ (**b**); the result "non-sky" image (**c**), and the histogram of its $J_{\min(R,\ G,\ B)}$ (**d**); original "sky" image (**e**), and the histogram of its $J_{\min(R,\ G,\ B)}$ (**f**); the result "sky" image (**g**), and the histogram of its $J_{\min(R,\ G,\ B)}$ (**h**).

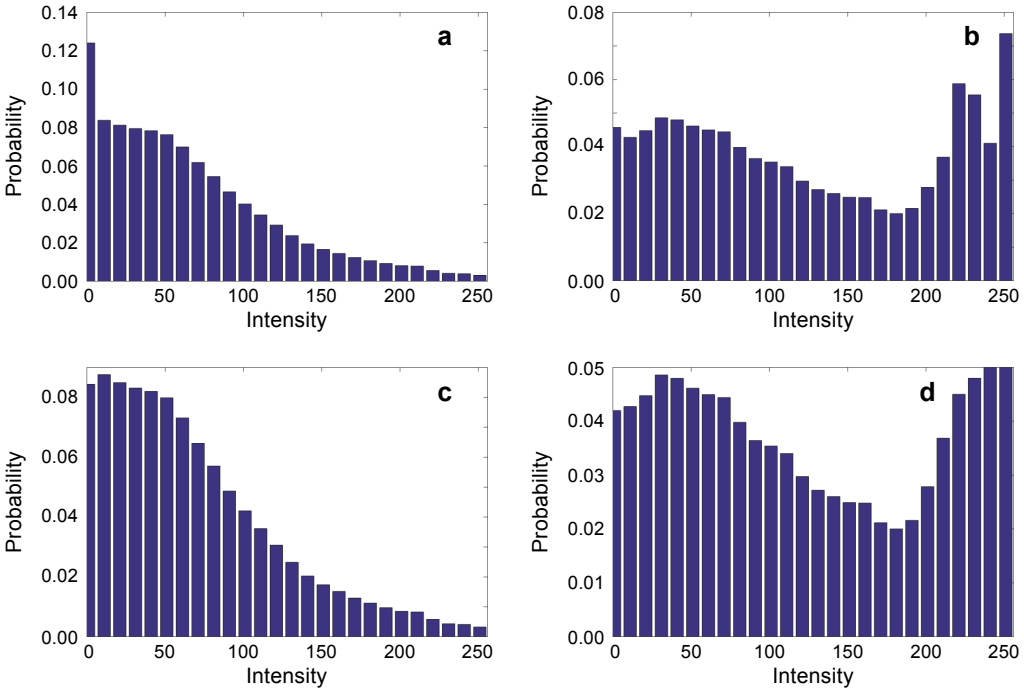

Fig. 2. Histogram of 100 non-sky photos (**a**), histogram of 100 outdoor photos with sky (**b**), the revised histogram of **a** (**c**), and the revised histogram of **b** (**d**).

fact, the area of sky would also influence the distribution of histogram. By changing the proportion of the high gray level, we can eliminate the influence.

In practice, after being processed by the histogram matching algorithm, the image is still blurred in a distant scene. Equation (8) shows that the influence of haze can be regarded as two parts. One is the direct attenuation $J_{\min(R,\,G,\,B)}t$ and the other is the air-light $A(1 - t)$. Because the air-light is an additive component, the histogram matching algorithm cannot remove it thoroughly. So before $I_{\min(R,\,G,\,B)}$ is processed by the histogram matching algorithm, we need to estimate the air-light and remove it from $I_{\min(R,\,G,\,B)}$.

Here we choose Gaussian filter to estimate the air-light and remove it from $I_{\min(R,\,G,\,B)}$ as follows:

$$J_{\min(R,\,G,\,B)}(x, y) = I_{\min(R,\,G,\,B)} - c_1\left(I_{\min(R,\,G,\,B)} * F(x, y)\right)^2 \tag{15}$$

where $F(x, y)$ is the Gaussian filter function, which can be replaced by other low-pass filter function; symbol $*$ denotes the convolution operator; c_1 is the correction coefficient which needs to be corrected according to the thickness of fog. After the removal

Fig. 3. Original image (**a**), the result only uses the histogram matching algorithm (**b**), and final result (**c**).

of the air-light, the results of histogram matching will be much clear. Combined with Eq. (15), Eq. (13) can be transferred into

$$I_{\mathrm{J}} = \frac{kA + H_{\mathrm{m}}\left[I_{\min(R,\,G,\,B)} - c_1\left(I_{\min(R,\,G,\,B)} * F(x, y)\right)^2\right]}{1 + k} \tag{16}$$

where H_{m} means the process of the histogram matching algorithm. Figure 3 shows the result.

3.2. Calculate the saturation component

After figuring out the intensity component, the value of the saturation component can be acquired by Eq. (12). Since the estimated intensity component is usually brighter than the actual value, we corrected the intensity component by a correction coefficient c_2. Because the intensity component can be very close to zero in some areas, the recovered saturation component S_{J} is prone to noise. So we restricted the intensity component by setting a lower bound I_0. The saturation component can be calculated as follows:

$$S_{\mathrm{J}} = k\left(\frac{A}{\max(c_2 I_{\mathrm{J}}, I_0)} - 1\right) \tag{17}$$

The typical value of c_2 is between 0.5 and 0.8, depending on the thickness of fog. And the typical value of I_0 is 0.03.

3.3. Recover the hazy image

In our model, there are only two unknown items, one is $J_{\min(R,\,G,\,B)}$ estimated by the histogram matching method and the other is atmosphere light A. If the value of atmosphere light A, which we estimated, is lower than the actual value, the results will appear as serious color distortion. But when the value is higher than the actual value, the results

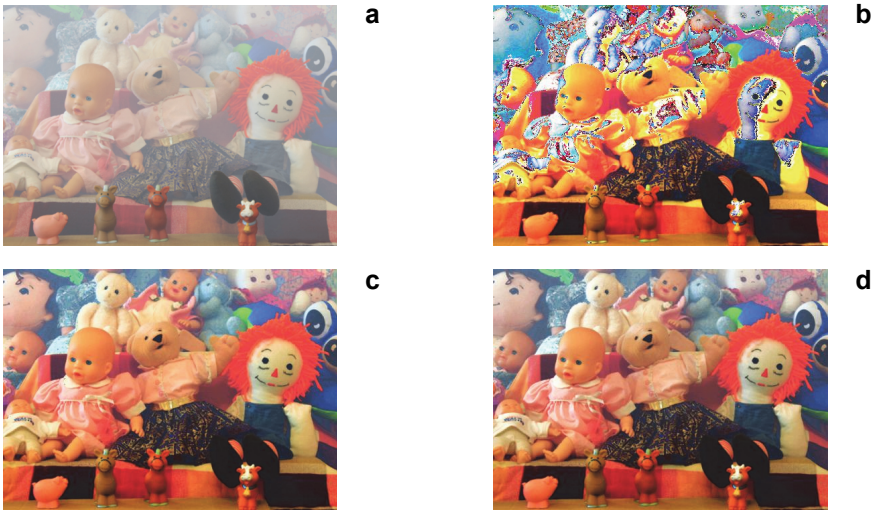

Fig. 4. Original image (**a**), the result with $A = 0.6$ (**b**), with $A = 0.9$ (**c**), and with $A = 1$ (**d**).

keep a nice visual effect. So we simply choose 1 as the value of atmosphere light. Figure 4 shows the results in different values of atmosphere light.

The final image is recovered by

$$\begin{cases} H_{\mathrm{J}} = H_I \\ S_{\mathrm{J}} = k\left(\dfrac{A}{\max(c_2 I_{\mathrm{J}}, I_0)} - 1\right) \\ I_{\mathrm{J}} = \dfrac{kA + H_{\mathrm{m}}\left[I_{\min(R,G,B)} - c_1\left(I_{\min(R,G,B)} * F(x,y)\right)^2\right]}{1+k} \end{cases} \tag{18}$$

In fact, when we recover a hazy image without the sky area, the image after the removal of haze will look dim. So we can increase the exposure of I_{J} for display. Figure 5 shows some final recovered images.

4. Experimental results

In our experiments, we used our dehazing method and the dark channel prior method to process different size images on a PC with a 3.3 GHz Intel Core i5-4590 CPU in Matlab. Compared with the dark channel prior, our method keeps a nature visual effect with a faster computing speed. Here we choose a guided filter to replace soft matting in the dark channel prior, which can increase the efficiency significantly and we take

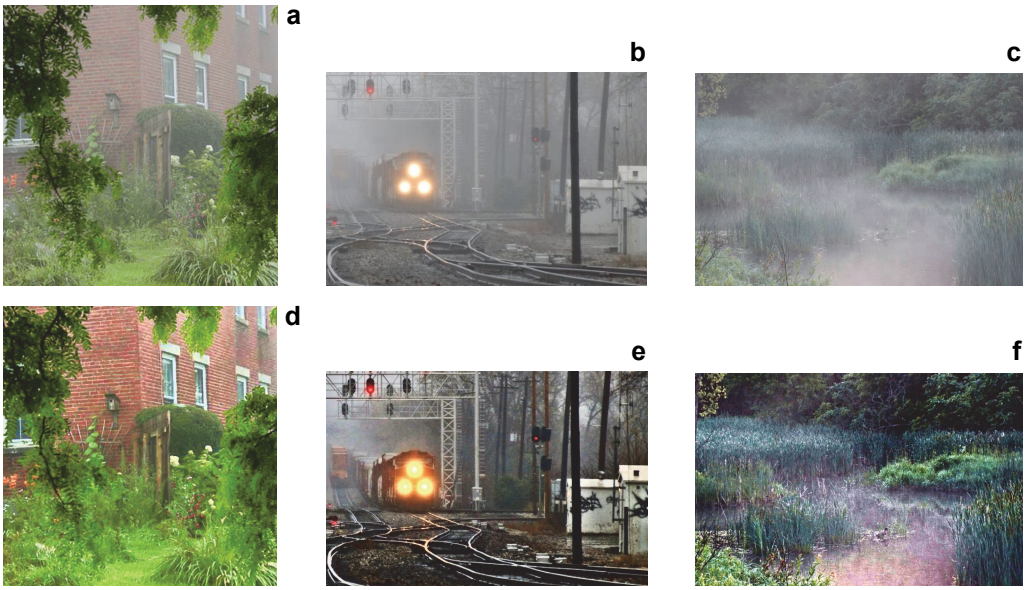

Fig. 5. Haze removal results. Input hazy images (**a**–**c**), and haze removal results (**d**–**f**).

Fig. 6. original images (**a**), dark channel prior (**b**), and our results (**c**).

T a b l e. The time cost of two methods.

Images	Image size [pixel]	Time [s]	
		Dark channel prior	Our method
Fig. 6**a**	1024 × 768	8.9683	0.254185
Fig. 6**b**	800 × 600	5.3612	0.160658
Fig. 6**c**	1024 × 768	8.9900	0.256236

15 × 15 patches to calculate the dark channel. The comparisons of two methods are shown in Fig. 6, and the cost time is shown in the Table. The results of both two methods are vivid, but the proposed method is much faster than the dark channel prior.

Figure 7 shows the results processed by different values of c_2. Apparently, the low value of c_2 might lead to over-saturation, and the high value of c_2 might lead to under -saturation. Actually, when the value of c_2 is between 0.5 and 0.8, we can achieve natural results. Figure 8 shows the results processed by different values of c_1. The results prove that the value of c_1 is related with the definition of distant area. A low value means an unclear scene while a high value means more details. However, color distortion may appear when the value is improperly high. The natural results will be achieved when c_1 is in the interval between 0.2 and 0.6.

Fig. 7. Original image (**a**), our result with $c_2 = 0.2$ (**b**), with $c_2 = 0.5$ (**c**), and with $c_2 = 1$ (**d**).

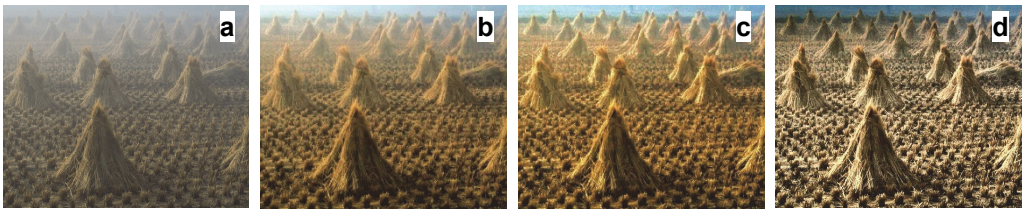

Fig. 8. Original image (**a**), with $c_1 = 0$ (**b**), with $c_1 = 0.5$ (**c**), and with $c_1 = 1$ (**d**).

In Figure 9 the influence of varying size of Gaussian filter has been taken into consideration. We conclude that the small size of Gaussian filter could lead to more thorough results, but it might cause an over enhancement in some area, and the halo effect would also appear in the sky area. Although the large size of Gaussian filter would reduce the halo effect and get a better overall visual effect, it would also lose lots of

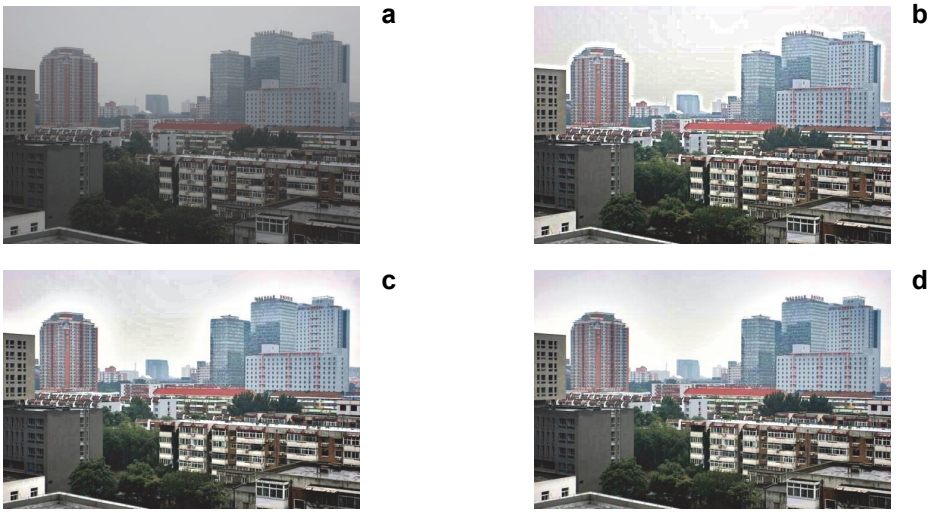

Fig. 9. Original image (**a**), our result with 30 × 30 size Gaussian filter (**b**), with 75 × 75 size Gaussian filter (**c**), and with 300 × 300 size Gaussian filter (**d**).

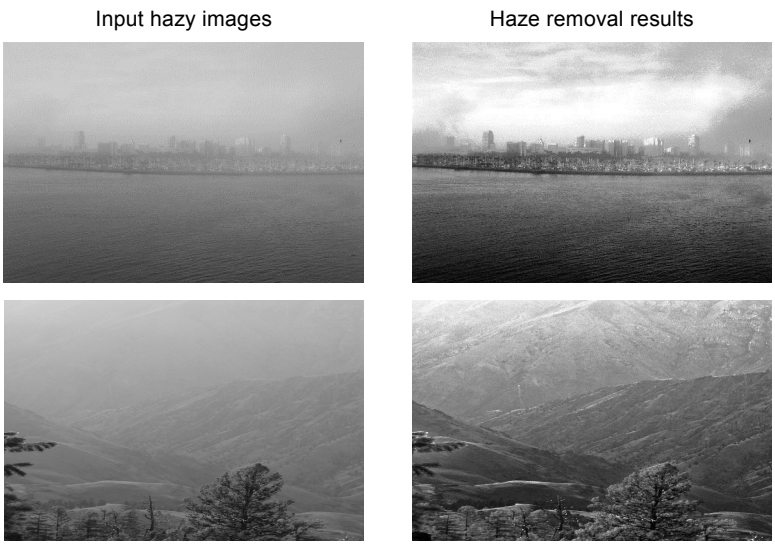

Fig. 10. Haze removal results in gray level images.

details. Because the halo effect only appears on the edge of the sky area, we can just ignore it, and choose a middle size Gaussian filter, such as a 75 × 75 size.

In fact, Eq. (17) can be taken separately to remove haze in gray level images. Figure 10 shows some processed results in gray images.

5. Conclusion

In this paper, we proposed a novel fog image degradation model in HSI color space. Based on this model, we used a statistical way to estimate the intensity component, and further got a haze-free image. The main advantage of the proposed method is its speed and vivid color. With its high efficiency, this method can be used as pre-processing in many systems. Actually, our method can be further promoted by using the improved histogram matching algorithm and some particular low-pass filters. Moreover, as our model shows a closely relationship between the intensity component and the saturation component, we plan to take our model as a standard to evaluate the color fidelity of a dehazing method.

Acknowledgements – This work was supported by the Natural Science Foundation of China (6180030017), the Natural Science Foundation of Guangdong Province (Grant Nos. 2015A030310278, 2016A030313473), the Key Technologies R&D Program of Guangzhou City (Nos. 201704020182, 201704020038, 201803030008), Water Resource Science and Technology Innovation Project of Guangdong Province (2017-23), and Supported by Hunan Province Key Laboratory of Videometric and Vision Navigation.

References

[1] NARASIMHAN S.G., NAYAR S.K., *Chromatic framework for vision in bad weather*, Proceedings IEEE Conference on Computer Vision and Pattern Recognition, CVPR 2000, Vol. 1, 2000, pp. 598–605.

[2] NARASIMHAN S.G., NAYAR S.K., *Contrast restoration of weather degraded images*, IEEE Transactions on Pattern Analysis and Machine Intelligence 25(6), 2003, pp. 713–724.

[3] NAYAR S.K., NARASIMHAN S.G., *Vision in bad weather*, Proceedings of the Seventh IEEE International Conference on Computer Vision, Vol. 2, 1999, pp. 820–827.

[4] SCHECHNER Y.Y., NARASIMHAN S.G., NAYAR S.K., *Instant dehazing of images using polarization*, Proceedings of the 2001 IEEE Computer Society Conference on Computer Vision and Pattern Recognition, CVPR 2001, Vol. 1, 2001, pp. I-325–I-332.

[5] SHWARTZ S., NAMER E., SCHECHNER Y.Y., *Blind haze separation*, 2006 IEEE Computer Society Conference on Computer Vision and Pattern Recognition (CVPR '06), Vol. 2, 2006, pp. 1984–1991.

[6] MUDGE J., VIRGEN M., *Real time polarimetric dehazing*, Applied Optics 52(9), 2013, pp. 1932–1938.

[7] SHUYIN TAO, HUAJUN FENG, ZHIHAI XU, QI LI, *Image degradation and recovery based on multiple scattering in remote sensing and bad weather condition*, Optics Express 20(15), 2012, pp. 16584–16595.

[8] CHIA-HUNG YEH, LI-WEI KANG, MING-SUI LEE, CHENG-YANG LIN, *Haze effect removal from image via haze density estimation in optical model*, Optics Express 21(22), 2013, pp. 27127–27141.

[9] FATTAL R., *Single image dehazing*, ACM Transactions on Graphics (TOG) 72(3), 2008, article ID 27.

[10] TAN R.T., *Visibility in bad weather from a single image*, 2008 IEEE Conference on Computer Vision and Pattern Recognition, 2008, pp. 1–8.

[11] KAIMING HE, JIAN SUN, XIAOOU TANG, *Single image haze removal using dark channel prior*, IEEE Transactions on Pattern Analysis and Machine Intelligence 33(12), 2011, pp. 2341–2353.

[12] KAIMING HE, JIAN SUN, XIAOOU TANG, *Guided image filtering*, [In] *Computer Vision – ECCV 2010. Lecture Notes in Computer Science*, [Eds.] K. Daniilidis, P. Maragos, N. Paragios, Vol. 6311, Springer, Berlin, Heidelberg, 2010, pp. 1–14.

[13] YANGYANG XIANG, SAHAY R.R., KANKANHALLI M.S., *Hazy image enhancement based on the full-saturation assumption*, 2013 IEEE International Conference on Multimedia and Expo Workshops (ICMEW), 2013, pp. 1–4.

Received November 19, 2017
in revised form January 11, 2018